Low-Temperature Deposition of TiO$_2$ Thin Films with Photocatalytic Activity from Colloidal Anatase Aqueous Solutions

Ana M. Peiró,[†] José Peral,[†] Concepción Domingo,[‡] Xavier Domènech,[†] and José A. Ayllón*,[†]

Departament de Química, Universitat Autònoma de Barcelona, 08193 Bellaterra, Spain, and Institut de Ciència de Materials de Barcelona, CSIC, 08193 Bellaterra, Spain

Crystalline TiO$_2$ films have been deposited on several substrates (glass, F-doped SnO$_2$-covered glass, and silicon wafers) by a drain-coating method from a colloidal anatase aqueous solution. The process is performed at low-temperature, 333 K, in open atmosphere. The colloidal TiO$_2$ consists on anatase nanoparticles of about 9 $\times$ 5 nm size, stabilized by tetrabutylammonium cations (TBA$^+$). This colloid has also been obtained under mild conditions (i.e., low temperature and ambient pressure) by hydrolysis of tetraisopropyl orthotitanate (TIP) in the presence of (TBA)OH and subsequent treatment by microwave radiation to enhance crystallization. Different film thicknesses have been obtained by consecutive deposition processes. Titania films thus obtained were transparent and showed good adherence. FT-IR analysis of the films reveal that TBA cations were not trapped in the film during the deposition process. No further thermal posttreatment was required to eliminate organics from the films or to induce titania crystallization. The photocatalytic activity of as-deposited titania has been assessed by the photodegradation of salicylic acid in aqueous solution under aerated conditions.

Introduction

Titanium dioxide has found extensive use in a great variety of applications. TiO$_2$ coatings are used in dye-sensitized photoelectrochemical cells,[1] as antireflection material in solar cells,[2] as gas sensors,[3] in photoelectrocatalysis,[4] and in photocatalysis.[5] In this latter case, the possibility of having the material supported on an inert substrate is especially interesting for wastewater and indoor atmospheres remediation[6] since problems derived from photocatalyst filtering are avoided. A variety of physical and chemical approaches have been used for TiO$_2$ thin-film preparation. Physical methods include sputtering,[7] CVD,[8] MOCVD,[9] light-induced CVD,[10] pulsed laser deposition,[11] ion-assisted electron-beam evaporation,[12] atomic layer deposition,[13] etc. These methods require a high amount of energy that is reemitted in part as exhaust heat or in the exhaust gases. Recently, efforts have been made to produce these films through chemical routes (wet methods), which are less energy consuming and do not require vacuum equipment. They include, among other, sol–gel methods,[14] electrochemical deposition,[15] Langmuir–Blodgett films,[16] and crystallization on functionalized surfaces.[17] A relatively simple and inexpensive chemical approach involves casting of thin films directly from colloidal semiconductor suspensions,[18] the main interest of these

* To whom all correspondence should be addressed. Telephone: (+34) 93 581 29 19. Fax: (+34) 93 581 29 20. E-mail: joseantonio.ayllon@uab.es.

† Universitat Autònoma de Barcelona.

‡ Institut de Ciència de Materials de Barcelona.

(1) (a) Thompson, D. W.; Kelli, C. A.; Farzad, F.; Meyer, G. *Langmuir* **1999**, *15*, 650. (b) Tennakone, K.; Senadeera, G. K. R.; Perera, V. P. S.; Kottegoda, I. R. M.; de Silva, L. A. A. *Chem. Mater.* **1999**, *11*, 2474. (c) Li, Y.; Hagen, J.; Schaffrath, W.; Otschik, P.; Haarer, D. *Sol. Energy Mater. Sol. Cells* **1999**, *56*, 167.

(2) (a) Gee, J. M.; Gordon, R.; Liang, H. http://www.sandia.gov/pv/comp/cells1.htm. (b) Doeswijk, L. M.; de Moor, H. H. C.; Blank, D. H. A.; Rogalla, H. *Appl. Phys. A* **1999**, *69*, S409.

(3) Lin, H. M.; Keng, C. H.; Tung, C. Y. *Nanostruct. Mater.* **1997**, *9*, 747.

(4) (a) Rodríguez, J.; Gómez, M.; Lindquist, S.-E.; Granquist, C. G. *Thin Solid Films* **2000**, *360*, 250. (b) Gerischer, H. *Electrochim. Acta* **1993**, *38*, 3. (c) Ichikawa, S.; Doi, R. *Thin Solid Films* **1997**, *292*, 130.

(5) Xagas, A. P.; Androulaki, E.; Hiskia, A.; Falaras, P. *Thin Solid Films* **1999**, *357*, 173.

(6) (a) Byrne, J. A.; Eggins, B. R.; Brown, N. M. D.; McKinney, B.; Rouse, M. *Appl. Catal., B* **1998**, *17*, 25. (b) Heller, A. *Acc. Chem. Res.* **1995**, *28*, 503. (c) Herrmann, J.-M.; Tahiri, H.; Ait-Ichou, Y. A.; Lassaletta, G.; González-Elipe, A. R.; Fernández, A. *Appl. Catal., B* **1997**, *13*, 219.

(7) (a) Mardare, D.; Tasca, M.; Delibas, M.; Rusu, G. I. *Appl. Surf. Sci.* **2000**, *156*, 200. (b) Suzuki, S. *Thin Solid Films* **1999**, *351*, 194.

(8) Lee, W. G.; Woo, S. I.; Kim, J. C.; Choi, S. H.; Oh, K. H. *Thin Solid Films* **1994**, *237*, 105.

(9) Kim, E. K.; Son, M. H.; Min, S. K.; Han, Y. K.; Wang, C. H.; Yom, S. S. *J. Appl. Phys.* **1996**, *79*, 4459.

(10) Halary, E.; Benvenuti, G.; Wagner, F.; Hoffmann, P. *Appl. Surf. Sci.* **2000**, *154–155*, 146.

(11) Escobar-Alarcón, L.; Haro-Poniatowski, E.; Camacho-López, M. A.; Fernández-Guasti, M.; Jímenez-Jarquín, J.; Sánchez-Pineda, A. *Appl. Surf. Sci.* **1999**, *137*, 38.

(12) Bhattacharyya, D.; Sahoo, N. K.; Thakur, S.; Das, N. C. *Thin Solid Films* **2000**, *360*, 96.

(13) Sammelselg, V.; Rosental, A.; Tarre, A.; Niinistö, L.; Heiskanen, K.; Ilmonen, K., Johansson, L.-S.; Uustare, T. *Appl. Surf. Sci.* **1998**, *134*, 78.

(14) (a) Jämting, Å.K.; Bell, J. M.; Swain, M. V.; Wielunski, L. S.; Clissold, R. *Thin Solid Films* **1998**, *332*, 189. (b) Lin, H.; Kozuka, H.; Yoko, T. *Thin Solid Films* **1998**, *315*, 111. (c) Nishide, T.; Mizukami, F. *Thin Solid Films* **1999**, *353*, 67.

(15) Natarajan, C.; Nogami, G. *J. Electrochem. Soc.* **1996**, *143*, 1547.

(16) Oswald, M.; Hessel, V.; Riedel, R. *Thin Solid Films* **1999**, *339*, 284.

films being their inherited properties from the native colloids such as photochromic,[19] photoelectrochemical,[20] and photocatalytic properties.[21] However, in these methods an annealing posttreatment, usually at 450 °C, is necessary to remove the organics used in the preparation of the colloidal suspension or paste. The thermal treatment also favors the adhesion of the titania to the substrate and increases the electric conductivity (the sheet resistance decreases) because of a better cohesion between particles.

It is evident the interest of low-temperature methods for fabrication of crystalline thin films of advanced materials[22] such as semiconductors, ceramics, or their composites and/or hybrids, not only from the point of view of energy saving, as annealing posttreatment is avoided, but also as they allow the use of low thermally resistant materials such as plastics, wood, or paper as substrates. Furthermore, to make the whole chemical approach environmental friendly, the use of aqueous solutions instead of organic solvents is desired.

Recently, our group has accomplished the deposition of anatase TiO_2 films with relative ease and at low-temperature using a new soft-solution processing method in which crystallization is enhanced by microwave heating.[23] In this paper we show a new method in which colloidal anatase is deposited on different substrates by a drain-coating process employing a colloidal aqueous solution at 333 K.

Experimental Section

Reagents. Chemicals were of reagent grade and were used without further purification: tetraisopropyl orthotitanate (TIP; Fluka); tetrabutylammonium hydroxide ((TBA)OH; 40% in water, Fluka); absolute ethanol (EtOH; Panreac); salicylic acid (Merck). The water employed in all preparations was purified by a Milli-Q system (Millipore).

Preparation of Aqueous Colloidal Solution. Anatase nanocrystals were prepared by the controlled hydrolysis of TIP as described previously,[24] with minor modifications. TIP (5 mL) was dissolved in absolute EtOH (30 mL), and the solution was added to a solution of 0.6 mL of (TBA)OH (40% in water) in 30 mL of absolute EtOH. Both solutions were preserved from atmosphere moisture before their mixture. Afterward, 185 mL of water was added. The obtained transparent solution, with a 19:1 Ti:TBA molar ratio, was heated to evaporate ethanol and 2-propanol (the TIP hydrolysis byproduct) until the volume of the solution was reduced to ca. 100 mL. This solution was heated to reflux for 2 h by means of a microwave furnace (Prolabo Maxidigest MX350) working at 60 W. After this

treatment, a transparent slightly blue-colored aqueous colloidal solution was recovered. Unless otherwise stated, a 5-fold diluted solution was used. To gain further knowledge, non MW-treated solutions, although not used in deposition experiments, were also studied. In both cases, solid samples for powder XRD characterization were obtained from aliquots dried at 333 K.

Substrates. Anatase nanoparticles were deposited on glass, F-doped SnO_2-covered glass (referred as TCO from now on) and Si(100) wafers. Glass slides were immersed both in boiling sulfuric acid and boiling Milli-Q water for 30 min, and afterward they were ultrasonically cleaned in acetone and absolute EtOH for 5 min. Finally, they were rinsed with water. TCO substrates with sheet resistance 15 Ω/□ (Flabeg, Pilkington Group) were ultrasonically cleaned in acetone and absolute EtOH for 5 min and rinsed with water. Si substrates were ultrasonicated in absolute EtOH and in acetone for 5 min. Afterward, Si substrates were rinsed with water and cleaned with diluted HF to dissolve silicon oxide. Finally, they were thoroughly rinsed with water.

Au: In the above paragraph, 4th sentence from the end, please check units for sheet resistance.

Deposition Method. For film preparation, the drain-coating method in which the substrate remains stationary while the solution is drained from the vessel was employed. Substrates were immersed for 5 min into 100 mL of the colloidal solution, which was maintained at 333 K in a thermostated vessel. Afterward, the solution level was lowered at a rate of 23 mm/min by means of a peristaltic pump connected to an open end in the bottom of the vessel. Upon removal from the solution, the substrate was carefully rinsed with water and dried under N_2 flow. Films so obtained were well-adhered. Adhesion was qualitatively evaluated by submerging the film in a beaker containing water and submitting to ultrasonic vibrations (Selecta, 50 W) for 5 min. No modification of the optical interference fringes was observed. TiO_2 layers on substrates could be thickened by means of consecutive drain-coating processes. In these experiments, substrates were immersed only for 1 min after the first draining process and were only rinsed with water and dried with N_2 at the end of the whole deposition process.

Characterization Techniques. Characterization of the dried colloid powder by X-ray diffraction (XRD) was carried out with a Rigaku Rotaflex RU-200B with Cu Kα radiation, operated at 50 kV and 80 mA over the range $10 < 2\theta < 60°$. Fluorescence spectra of the TiO_2 colloidal solutions were recorded on a Perkin-Elmer LS 50 luminescence spectrometer at room temperature; an excitation wavelength of 252 nm was employed. For TEM studies, a drop of 10-fold-diluted colloidal solution was directly deposited on carbon-coated copper grids. Observations were made with a Philips CM30 microscope working at 300 kV. Fourier transform infrared spectra (FTIR) of TiO_2 nanocrystallites onto Si substrates were recorded in a Perkin-Elmer System 2000 FT-IR. Optical absorption spectra (UV–vis) of colloidal solutions and films on glass and TCO substrates were recorded in the absorption mode using a Hewlett-Packard diode array spectrometer (model 8453) at a resolution of 1 nm. Grazing-angle X-ray diffraction patterns of the deposited films were recorded on a Siemens D-3400 apparatus operated at 40 kV and 30 mA. The diffraction data were recorded at different X-ray incidence angles over the range $15 < 2\theta < 60°$.

Photocatalysis. The photoactivity of TiO_2 films on glass slides was evaluated by the degradation of salicylic acid under UV illumination. Experiments were conducted in a thermostated cylindrical Pyrex cell of 130 cm^3 capacity in which temperature was kept at 298 K. A 125 W Philips HPK medium-pressure mercury vapor lamp was used as light source. A 6.25×10^{-5} mol L^{-1} salicylic acid solution (100 mL) was employed. Films for photocatalytic experiments were prepared by 25 consecutive drain-coating processes, resulting approximately in 2×10^{-2} mg TiO_2 cm^{-2}. The solution inside the cell was stirred, and air was bubbled into it during the whole experiment. Absorbance of initial and irradiated samples was determined with a Philips PU 8620 UV/vis/NIR spectro-

(17) (a) Xiao, Z.; Gu, J.; Huang, D.; Lu, Z.; Wei, Y. *Appl. Surf. Sci.* **1998**, *125*, 85. (b) Shin, H.; Collins, R. J.; de Guire, M. R.; Heuer, A. H.; Sukenik, C. N. *J. Mater. Res.* **1995**, *10*, 692. (c) Kovtyukhova, N.; Ollivier, P. J.; Chizhik, S.; Dubravin, A.; Buzaneva, E.; Gorchinskiy, A.; Marchenko, A.; Smirnova, N. *Thin Solid Films* **1999**, *337*, 166.

(18) Kamat, P. V. *Chemtech* **1995**, June, 22.

(19) Torimoto, R.; Fox, R. J., III; Fox, M. A. *J. Electrochem. Soc.* **1996**, *143*, 3712.

(20) (a) Hagfeldt, A.; Björkstén, U.; Lindquist, S.-E. *Sol. Energy Mater. Sol. Cells* **1992**, *27*, 293. (b) Kozuka, H.; Takahashi, Y.; Zhao, G.; Yoko, T. *Thin Solid Films* **2000**, *358*, 172.

(21) Zeltner, W. A.; Hill, Jr. C. G.; Anderson, M. A. *Chem. Technol.* **1994**, 21.

(22) Yoshimura, M. *J. Mater. Res.* **1998**, *13*, 796.

(23) (a) Vigil, E.; Saadoun, L.; Ayllón, J. A.; Domènech, X.; Zumeta, I.; Rodríguez-Clemente, R. *Thin Solid Films* **2000**, *365*, 12. (b) Vigil, E.; Saadoun, L.; Rodríguez-Clemente, R.; Ayllón, J. A.; Domènech, X. *J. Mater. Sci. Lett.* **1999**, *18*, 1067. (c) Vigil, E.; Ayllón, J.; Peiró, A. M.; Rodríguez-Clemente, R.; Domènech, X.; Peral, J. *Langmuir* **2001**, *17*, 891.

(24) Saadoun, L.; Ayllón, J. A.; Jiménez-Becerril, J.; Peral, J.; Domènech, X.; Rodríguez-Clemente, R. *Mater. Res. Bull.* **2000**, *35*, 193.

photometer at a wavelength of 296 nm, using a quartz cuvette of 4 cm of optical path length.

Results and Discussion

Anatase TiO₂ Colloid Characterization. Preliminary work has shown that (TBA)OH can be used as hydrolysis control agent for the production of anatase TiO₂ from titanium alcoxides.[24] When an alcoholic solution of TIP is mixed with a mostly alcoholic (TBA)-OH solution (obtained from the dilution of a concentrated aqueous solution of (TBA)OH in a relatively large amount of absolute ethanol), the precipitation of titanium hydroxide does not take place even when a great amount of water is added afterward, and transparent colloidal solutions are obtained. Other ways of using a tetraalkylamonium hydroxide ((TAA)OH) for the synthesis of TiO₂ are described in the literature.[25−27] In these works a titanium alkoxide precursor is first hydrolyzed by water yielding an amorphous precipitate of titanium hydroxide, and a (TAA)OH, often tetramethylammonium hydroxide, is added afterward to control further peptization and crystallization, which are achieved by relatively severe processes such as autoclaving[26,27] or prolonged reflux treatment.[25, 27]

In our case, a faster treatment, such as microwave irradiation for 2 h, is used to enhance the crystallization of the titania precursor. Previous to MW treatment, most alcohols from the mixture are eliminated by evaporation. This step allows one to raise by some degrees Celsius the refluxing temperature of the solution during microwave treatment and, particularly, gives an aqueous solution that can be more easily manipulated, as no organic vapors are produced. In addition, it has been reported that water favors crystallinity of titania, while alcohol presents the contrary effect.[28]

In this work colloidal TiO₂ was prepared by following our previously described method[24] but with a 19:1 Ti:TBA molar ratio instead of the 10:1 ratio reported. This change was made to reduce the content of organics in the colloidal solution. Although titania growth control is necessary, the presence of organics in the final product is very undesirable. However lower concentrations of (TBA)OH did not show a full stabilizing effect.

To characterize the crystal structure of TiO₂ nanoparticles in the colloidal solution, 30 mL of colloid was evaporated at 333 K, yielding a bright water-dispersible yellow solid which was examined by XRD. Figure 1a shows the XRD pattern of this solid, in which broad peaks are observed at values of 2θ equal to 25.6, 38.1, 48.2, and 54.7° that correspond to the anatase structure. An small broad signal at 31° (arrow) is ascribed to TiO₂ brookite traces. No differences were observed between XRD patterns of samples evaporated immediately after colloid preparation or 20 days later. Indeed, colloidal solutions were kept at room temperature in closed
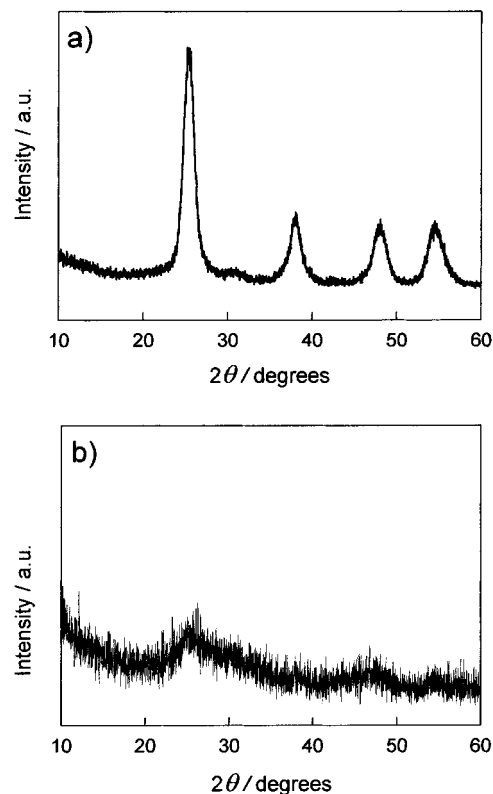

Figure 1. X-ray diffraction patterns of TiO₂ crystallites obtained after evaporating the colloidal solution at 333 K: (a) after and (b) before MW treatment.

vessels for several months without any change being observed. The pH of these solutions is close to 10.5, a value certainly higher than PZC (point zero charge) values reported for TiO₂.[29] At this pH, nanoparticles are negatively charged. Indeed, it is well-known that a strong base as (TBA)OH favors the formation of Ti−O⁻ groups on the TiO₂ surface. [27,30] TBA cations supply the counteracting positive charge. To assess the effect of MW, further experiments with non-MW-treated solutions were performed. Figure 1b shows the XRD pattern of the solid recovered after evaporation at 333 K of non-MW-treated colloid. Only a very broad signal centered at ca. 24−28° is observed. This fact suggest that TiO₂ crystallites have a very small size, which must be about 1 nm. [31]

Morphology and size of colloidal nanoparticles after MW treatment were examined by transmission electron microscopy (TEM). Figure 2 shows elongated box-shaped particles with a particle size distribution of about 7−11 nm length and 3−6 nm width.

Figure 3shows the UV−vis spectra of the colloidal solution before and after MW treatment. There is no optical absorption at $\lambda > 370$ nm, suggesting that the slight blue color may result from the luminescence of the colloids;[32] some contribution due to the Tyndall effect cannot be discarded. These spectra were processed in order to obtain the energy band gap, E_g, from the

(25) Moritz, T.; Reiss, J.; Diesner, K.; Chemseddine, A. *J. Phys. Chem. B* **1997**, *101*, 8052.

(26) Burnside, S. D.; Shklover, V.; Barbé, C.; Comte, P.; Arendse, F.; Brooks, K.; Grätzel, M. *Chem. Mater.* **1998**, *10*, 2419.

(27) Chemseddine, A.; Moritz, T. *Eur. J. Inorg. Chem.* **1999**, 235.

(28) Yin, S.; Inoue, Y.; Uchida, S.; Fujishiro, Y.; Sato, T. *J. Mater. Res.* **1998**, *13*, 844.

(29) Kormann, C.; Bahnemann, D. W.; Hoffmann, M. R. *J. Phys. Chem.* **1988**, *92*, 5196.

(30) Livage, J.; Henry, M.; Sanchez, C. *Prog. Solid State Chem.* **1998**, *18*, 259.

(31) Monticone, S.; Tufeu, R.; Kanaev, A. V.; Scolan, E.; Sanchez, C. *Appl. Surf. Sci.* **2000**, *162−163*, 565.

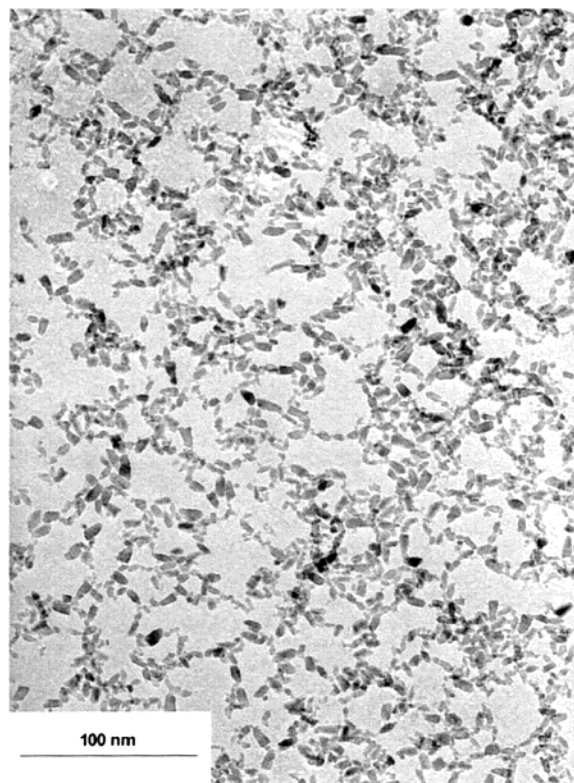(32) Liu, Y.; Claus, R. O. *J. Am. Chem. Soc.* **1997**, *119*, 5273.

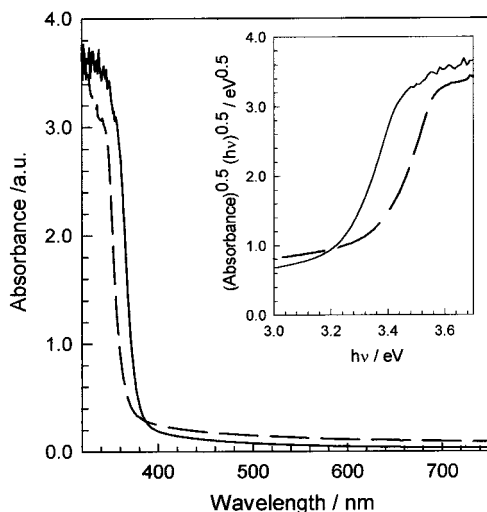**Figure 2.** TEM images corresponding to anatase nanocrystallites after MW treatment.

Figure 3. UV–vis spectra of anatase colloid solution: (dashed line) before and (solid line) after MW treatment. Insert: Variation of (absorbance)$^{0.5}(h\nu)^{0.5}$ with excitation energy ($h\nu$) for the anatase colloid to identify indirect transitions.

expression corresponding to indirect gap semiconductors (insert in Figure 3):

$$\alpha(h\nu)\,h\nu \propto (h\nu - E_{g})^{2}$$

Here α is the absorption coefficient (cm^{-1}) and $h\nu$ (eV) is the energy of excitation. From these plots, a value of E_{g} of 3.28 eV is obtained for the colloid after MW treatment, which is ascribed to bulk anatase (3.18 eV),[33] and a value of 3.41 eV for colloid before MW treatment.
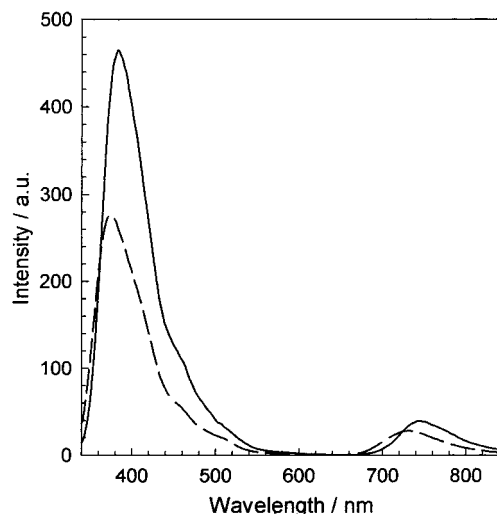

Figure 4. Fluorescence spectra of the anatase colloid at two stages of the preparation: (dashed line) before and (solid line) after MW treatment. In the later case the intensity of spectra has been 10-fold divided to facilitate comparisons. Experimental conditions: room temperature; excitation wavelength = 252 nm.

In this latter case, an increase of the band gap energy, and therefore a blue shift in the absorption edge, is in accordance with the effects of quantization with decreasing particle size that have been accounted in several studies for very small TiO_2 colloid particles (d < 4 nm)[34] and even for larger particles (d < 10.8 nm).[35]

To further characterize the TiO_2 colloidal solution, fluorescence spectra were recorded at various stages of the preparation. Figure 4 shows the fluorescence spectra of the colloidal solution before and after MW irradiation. Bands with a broad spectral width were observed in both cases. For MW-treated colloids (solid line), a sharp increase after 340 nm is observed, reaching a maximum at 384 nm. As in refs 32 and 36, most of the fluorescence of the colloidal TiO_2 takes place in the blue portion of the visible spectrum and diminishes toward the green portion of the spectrum. The emission maximum corresponds to the band gap (3.23 eV) of the bulk semiconductor. Single-crystal semiconductors show a sharp emission maximum corresponding to the band gap. On the contrary, the spectrum has a half-width of ca. 61 nm and tails up to 562 nm, this broad emission being typical of semiconductor-particle suspensions in water. Fluorescence between 600 and 900 nm is associated with transitions of electrons from the conduction band edge to holes trapped at an interstitial Ti^{3+} site.[37] Fluorescence spectrum recorded before MW irradiation (dashed line) presents a similar shape to that of the irradiated colloid but its intensity is less than 1/10. In addition, a blue shift displacement of approximately 10 nm in the whole spectrum is observed. These results suggest that incipient tiny nucleous of crystalline TiO_2

(33) Serpone, N.; Lawless, D.; Khairutdinou, R. *J. Phys. Chem.* **1995**, *99*, 16646

(34) (a) Choi, V.; Termin, A.; Hoffmann, M. R. *J. Phys. Chem.* **1994**, *98*, 13669. (b) Bahnemann, D. W. *Isr. J. Chem.* **1992**, *33*, 115. (c) Joselevich, E.; Willner, I. *J. Phys. Chem.* **1994**, *98*, 7628. (d) Anpo, M.; Shima, T.; Kodama, S.; Kubokawa, Y. *J. Phys. Chem.* **1987**, *91*, 4305.
(35) Sun, F.; Wu, M.; Li, W.; Li, X.; Gu, W.; Wang, F. *Cuihua Xuebao* **1998**, *19*, 3229.
(36) Chandrasekaran, K.; Thomas, J. K. *J. Chem. Soc., Faraday Trans.* **1984**, *80*, 1163.
(37) Samtsov, M. P. *J. Electroanal. Chem.* **1992**, *340*, 73.

must be present, although not being detectable by XRD (amorphous TiO_2 colloids do not show fluorescence).[36]

As a conclusion, particles exhibiting quantum-sized effects (blue-shift in UV−vis and fluorescence spectra) are obtained before MW treatment of the colloidal solution. To enhance the growth of these particles, and hence to obtain particles with bulk properties, which require less energy to promote an electron from the valence band to the conduction band, a MW irradiation treatment is performed, which yields the desired stable colloidal solution.

Anatase TiO_2 Thin-Film Characterization. TiO_2 nanoparticles were deposited onto different substrates, such as glass, silicon, and TCO, by a drain-coating method performed at 333 K. To assess if layer thickness was dependent upon the time of immersion of substrates in the colloidal solution previous to the draining process, several experiments were performed at different times of immersion ranging from 5 to 60 min, before draining at the same rate. No significative differences in UV−vis spectra of these layers were observed. This fact suggests that deposition of TiO_2 onto the substrates does not take place in the solution bulk. However, it was observed that the draining rate clearly affects the homogeneity of the films. Hence, it is inferred that deposition takes place when the solution drains near the interface between the aqueous solution, the glass substrate, and the air, i.e., at the meniscus. Actually, homogeneous films were only obtained when a uniform movement of such interface was achieved. It has been observed that deposited films do not disperse in water, while the solid sample obtained after evaporation of the colloidal solution on the substrate could be redispersed in water, both processes being performed at the same temperature. The redispersion of the solid obtained after simple evaporation could be explained considering that the junction among anatase nanocrystals is hindered by their surface negative charge due to adsorbed hydroxyl anions and by the presence of TBA cations. Further, the films obtained by the drain-coating process are well-adhered, as denoted by their resistance to ultrasonic vibrations. These facts account for some other mechanism taking place in the meniscus rather than simple evaporation of the colloidal solution onto the substrate.

A first hypothesis for the mechanism of film formation was that neutral TiO_2 nanocrystals were deposited in the meniscus. This fact would imply that no TBA cations are present in films, as nanoparticles lose their excess hydroxyl groups, which remain in solution together with their corresponding TBA counteracting cations (see detailed explanation below). To confirm the lack of TBA cations in films, FT-IR spectra were analyzed for films deposited onto Si(100). On one hand, a drop of diluted aqueous colloidal solution was evaporated onto Si(100); the FTIR spectrum (Figure 5a) revealed several peaks assignable to TBA cations (i.e. 2967, 1485, 1369 cm^{-1}), as well as a broad band corresponding to bulk TiO_2 skeletal frequency region (below 730 cm^{-1}).[38] The presence of water was also manifested. On the other hand,
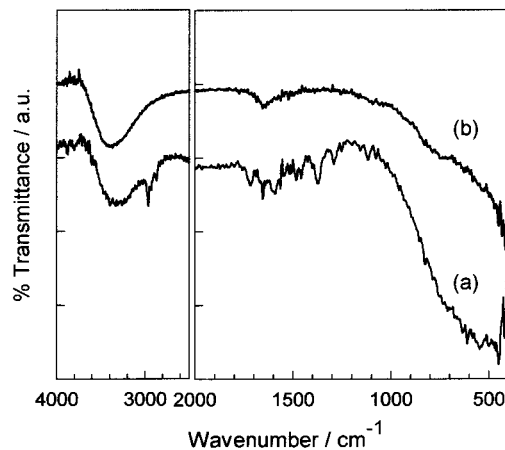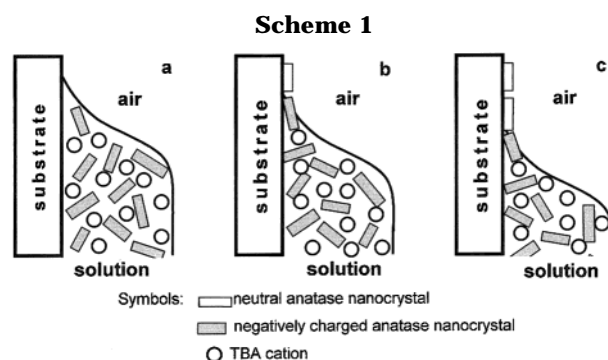

Figure 5. FTIR spectra of anatase colloid solution deposited on Si substrates: (a) a drop of colloidal solution deposited and then evaporated; (b) deposition performed by the drain-coating method.

Scheme 1

a 6-fold drain-coated Si(100) sample was studied. The FT-IR spectrum of this sample shows only tiny peaks corresponding to organic compounds (Figure 5b), while the presence of TiO_2 is clearly denoted by the absorbance in the region below 800 cm^{-1}.[38] Therefore, it was concluded that TiO_2 nanocrystallites deposited by the drain-coating method are mainly free of TBA cations. To explain such an experimental finding, a tentative simplified mechanism is proposed (see Scheme 1), in which liquid−solid and liquid−air interfaces are represented. Scheme 1a shows the colloidal solution, consisting of negatively charged anatase nanoparticles stabilized by tetrabutylammonium cations (TBA^+), in contact with the substrate surface. Scheme 1b shows the situation once the solution level has been lowered and, hence, the deposition process has started. Some TiO_2 crystallites have been deposited onto the substrate surface. We suggest that when anatase nanocrystals at the meniscus anchor to the substrate, they become neutral; their excess of negative charges is lost as hydroxyl anions. Then, these OH^- anions and, consequently, TBA^+ counterions are drawn to the solution. Classic models concerning surface tension of electrolyte solutions state that charged inorganic species tend to avoid the air−water interface and concentrate in the solution bulk.[39] However, recent ab initio calculation on NaCl solutions in water show that ions do not uniformly distribute in the air−water interface; chloride anions actually accumulate near the water surface.[40]

(38) (a) Harizanov, O.; Harizanova, A. *Sol. Energy Mater. Sol. Cells* **2000**, *63*, 185. (b) Kaliwoh, N.; Zhang, J.-Y.; Boyd, I. W. *Surf. Coat. Technol.* **2000**, *125*, 424. (c) González, R. J. Ph.D. Thesis, Virginia Polytechnic Institute, Blacksburg, VA, 1996.

(39) Levine, I. N. *Physical Chemistry*, 4th ed.; McGraw-Hill: New York, 1996; Vol. 1, p 391.
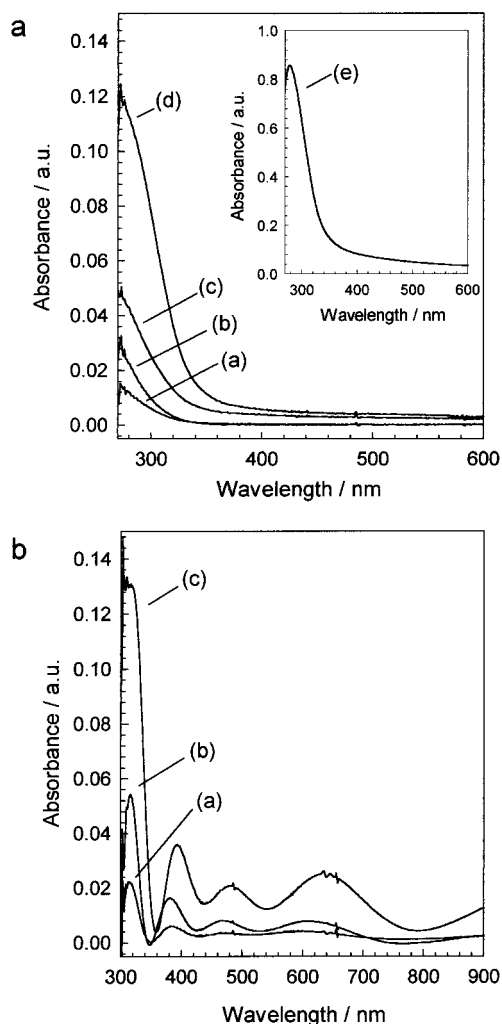
a

b

Figure 6. (a) UV−vis spectra of TiO$_2$ layer on glass substrates after (a) 1, (b) 10, (c) 15, (d) 20, and (e) 25 (insert) drain-coating processes with anatase colloid. (b) UV−vis spectra of TiO$_2$ layer on TCO substrates after (a) 1, (b) 5, and (c) 15 drain-coating processes with anatase colloid.

The good adherence of the film to the substrate suggests that strong joining forces act between the substrate and the deposited crystallites. Strong covalent oxo bridges (>X−O−Ti<; X = Si, Sn) could account for the good adherence reported.

The thickness of the TiO$_2$ layer as a function of the number of repeated deposition processes was studied. The thinnest layers were transparent and colorless, while in the thickest ones interference colors were observed. Figure 6a shows the UV−vis absorption spectra of films deposited on glass after 1, 10, 15, 20, and 25 drain-coating processes, respectively. This figure shows that absorption, and consequently the thickness of the layer, are enhanced when the number of deposition processes increases.

The amount of TiO$_2$ deposited in each process is small, as estimated by gravimetry: a 25-fold drain-coated glass substrate contains approximately 2×10^{-2} mg of TiO$_2$ cm^{-2}, i.e., a layer thickness of 54 nm, considering the whole layer as being compact. In fact, this is a minimum value as a porous layer rather than a compact one is obtained by the actual mechanism of deposition. This
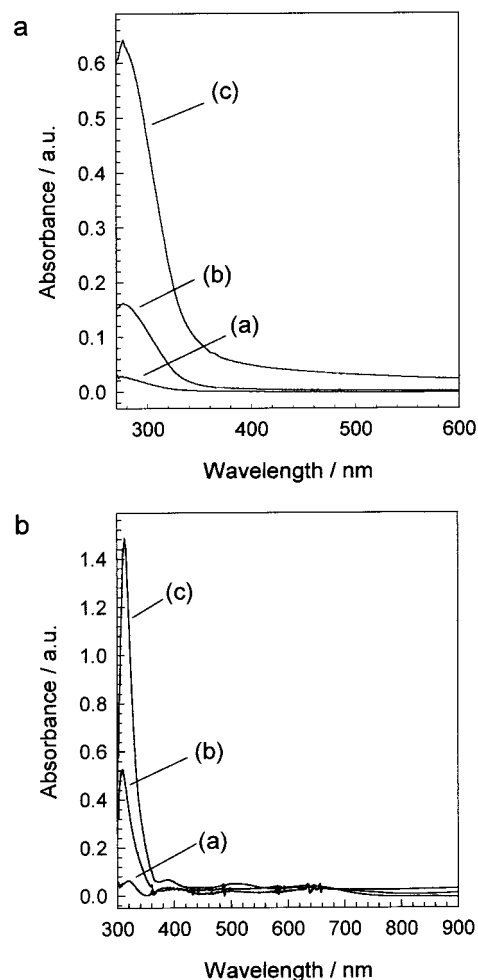
(40) Jungwirth, P.; Tobias, D. J. *J. Phys. Chem. B* **2000**, *104*, 7702.

a

b

Figure 7. (a) UV−vis spectra of TiO$_2$ layer on glass substrates after (a) 1, (b) 10, and (c) 15 drain-coating processes with concentrated anatase colloid solution. (b) UV−vis spectra of TiO$_2$ layer on TCO substrate after (a) 1, (b) 10, and (c) 15 drain-coating processes with concentrated anatase colloid solution.

means that, at least, about 2 nm of layer is deposited in each coating, yielding a submonolayer coverage (as confirmed by AFM). On subsequent coating processes, the previously deposited anatase crystallites act as substrate. In this case the anchorage is favored as homojunctions are more easily formed than heterojunctions. This fact explains the faster growth in thickness with an increasing the number of drain-coating processes (see Figure 6a).

From UV−vis spectra, the corresponding E_g values could be determined. Indeed, calculated values for the thinnest films were higher than expected due to experimental limitations related to the employed technique. However, for films produced after at least 15 drain-coating processes, band gap values correspond to bulk TiO$_2$ anatase. Figure 6b shows the UV−vis absorption spectra of films deposited on TCO after 1, 5, and 15 drain-coating processes. Absorption maxima increments with the number of drain-coating processes were more pronounced for layers deposited onto TCO than onto glass.

Figure 7 shows UV−vis absorption spectra of films deposited after 1, 10, and 15 drain-coating processes with concentrated colloid solution onto glass (Figure 7a) and onto TCO substrate (Figure 7b). Thicker layers were
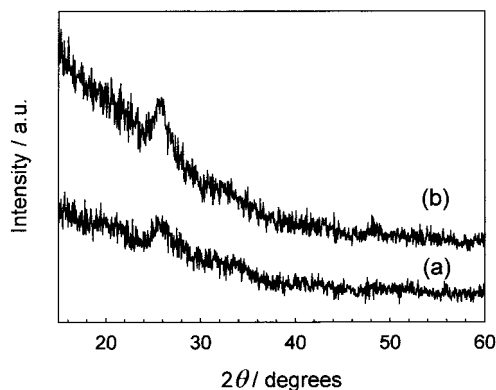
Figure 8. X-ray diffraction pattern of TiO_2 layer on glass after 1 and 10 drain-coating processes with anatase colloid (bottom and top, respectively).
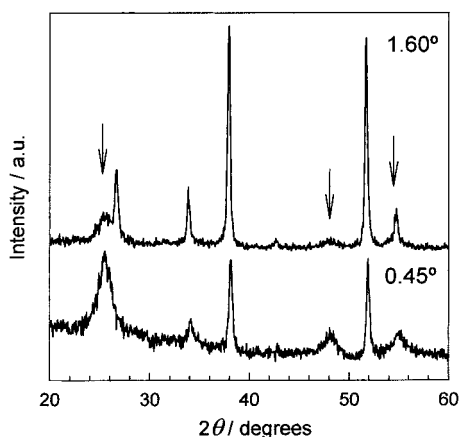

Figure 9. Grazing-angle XRD pattern of TiO_2 layer on TCO after 15 drain-coating processes with anatase colloid at two different grazing incidence angles: 0.45 and 1.60° (top and bottom, respectively). For an angle of incidence of 0.45°, TiO_2 anatase peaks are observed (marked with an arrow), as well as peaks corresponding to the substrate. For 1.60°, the depth of X-ray penetration into the film is higher and peaks corresponding to the substrate are more intense.

obtained from concentrated colloidal solution compared to diluted ones for the same number of deposition processes. Moreover, again a more pronounced absorbance increase for layers deposited onto TCO compared to glass is observed. The fact that TiO_2 nanoparticles are more easily deposited onto TCO than onto glass can be explained by considering that the crystalline nature of the TCO surface induces a faster growth of the TiO_2 layer, compared with the amorphous surface of glass.

XRD experiments were performed to further confirm the crystallinity of the deposited materials, which had already been inferred by the optical properties of the films. Figure 8 shows the X-ray diffraction pattern of TiO_2 layers on glass after 1 and 10 drain-coating processes with anatase colloid. Broad peaks were observed for the thickest layers which were assigned to anatase structure. It was not possible to characterize the thinnest layers by XRD. For films formed onto TCO, anatase structure was also found (see Figure 9).

Photocatalysis with the TiO₂ Thin Films. The photocatalytic activity of the films toward the degradation of salicylic acid in aqueous solutions was investigated. Figure 10 shows the percentage of salicylic acid
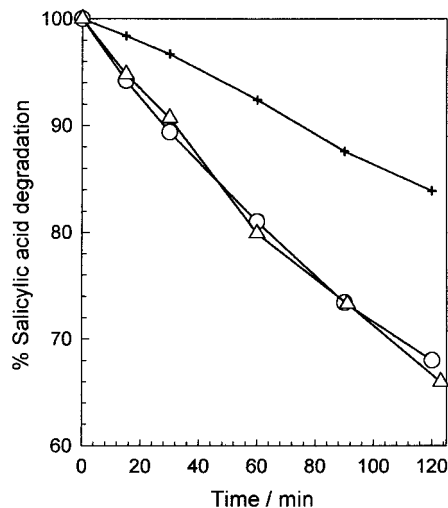

Figure 10. Percentage of salicylic acid removed with irradiation time for aqueous suspensions (6.25×10^{-5} mol L^{-1}; 100 cm^3) in the presence of nanocrystalline anatase films prepared by 25 consecutive drain-coating processes (ca. 2×10^{-2} mg TiO$_2$ cm^{-2}). Experimental conditions: UV irradiation; 298 K; stirred; air was bubbled. Key: (+) clean substrate; (○) films without thermal treatment; (△) films with thermal treatment (675 K, 2 h).

degraded as a function of irradiation time for different treated TiO_2 films. As previously reported, titania powders obtained from a similar aqueous colloidal solution with a Ti:TBA 10:1 molar ratio presented photocatalytic activity in the gas-phase oxidation of formaldehyde after calcination to eliminate TBA cations.[24] In the present study, however, no annealing posttreatment was necessary to eliminate TBA cations, as they were not present in deposited TiO_2 films. For photocatalytic essays, 25-fold drain-coated glass substrates were used. Figure 10 shows the results of photocatalytic activity of two TiO_2 films, (i) an as-deposited film not annealed and (ii) a heat-treated sample at 675 K for 2 h. As can be seen, no difference in the degradation rate is found between both samples; this fact implies that no annealing treatment is necessary in the present case to induce crystallinity in samples in order to improve photocatalytic activity, as is the general case.[41] It must be signaled that after these experiments no loss in the photocatalytic activity of films was detected.

In conclusion, it has been shown that nanocrystalline TiO_2 anatase stabilized by (TBA)OH can be deposited onto different substrates with a method performed at low temperature, yielding photoactive material for the degradation of a liquid-phase contaminant.

(41) Pozzo, R. L.; Baltanás, M. A.; Cassano, A. E. *Catal. Today* **1997**, *39*, 219.